Future Energy
Open Access Journal
ISSN 2832-0328

May 2022| Volume 01 | Issue 01 | Pages 16-23

Journal homepage: https://fupubco.com/fuen

https://doi.org/10.55670/fpll.fuen.1.1.11

Future Publishing LLC

Article

Analysis of high voltage shunt capacitor bank over-voltage breakdown detection

Mohsen Rajabali Pour[1], Mohammad Azimian[2]*

[1]Malaysia-Japan International Institute of Technology, Universiti Teknologi Malaysia, Jalan Sultan Yahya Petra, 54100, Kuala Lumpur, Malaysia
[2]Engineering Department, Razak Faculty of Technology and Informatics, Universiti Teknologi Malaysia, Jln Sultan Yahya Petra, 54100, Kuala Lumpur, Malaysia

ARTICLE INFO

Article history:
Received 10 March 2022
Received in revised form
11 April 2022
Accepted 17 April 2022

Keywords:
Shunt capacitor banks, Component aging over-voltage breakdown, Detection method Mallet algorithm

Corresponding author
Email address: mazimian82@gmail.com

DOI: 10.55670/fpll.fuen.1.1.11

ABSTRACT

The traditional over-voltage breakdown detection method ignores the suppression of the inrush current of over-voltage breakdown, resulting in low over-voltage signal detection accuracy and a large detection deviation. As a result, a method is proposed for detecting and analyzing the ageing over-voltage breakdown of high voltage shunt capacitor banks. The breakdown model of aged components of the container group is built to determine the breakdown time of the container's overvoltage. Based on this, the annual load of the capacitor bank's aged component material is evaluated, and data on over-voltage breakdown strength is collected. The Mallet algorithm is used to decompose and convert strength data into electrical signals. The high voltage shunt capacitor's over-voltage breakdown inrush current suppressor is built by combining the second-order under damping circuit and the voltage divider. Based on this, the parameters of HV shunt capacitor overvoltage breakdown are obtained, and the detection of HV shunt capacitor overvoltage breakdown of aged HV shunt capacitor banks is completed. The simulation results show that the proposed detection method's over-voltage breakdown output is in perfect agreement with the monitoring device's actual output and has ideal application performance.

1. Introduction

Capacitor faults in substations occur frequently, which pose a great threat to the safe operation of the power grid and cause great economic losses to power enterprises. The failure of shunt capacitors is related to the manufacturing level, operating conditions, and the reliability of the control protection device. The correct analysis of capacitor faults and the reduction of faults, and the improvement of grid reliability is of great importance to the improvement of economic benefits of power enterprises and the society [1-2]. Therefore, some good research results have been obtained for the breakdown detection of aged over-voltage of HV shunt capacitor banks in related fields. In literature [3], the over-voltage dynamic control method of circuit breaker was proposed to detect the over-voltage breakdown of aged capacitor banks. Develop capacitor overvoltage breakdown strategy. The dynamic puncture characteristics of the contact gap of the shunt capacitor during the over-voltage phase are obtained by using the puncture characteristics measuring device. According to the dispersion of the over-voltage time between the capacitor and the shunt capacitor, the corresponding control strategy of the over-voltage breakdown of the capacitor is developed. This method is difficult to suppress the over-voltage inrush and easy to cause the damage to capacitor equipment in actual operation. Literature [4] is analyzed the capacitor group of internal components in the process of running through a string, the second string, and the breakdown of discharge voltage of fault phase capacitor transient variation. The peak value of discharge current is estimated. In the EMTP simulation software to establish the breakdown model of the capacitor, calculated and analyzed the breakdown of the element equivalent circuit parameters on the influence of the peak discharge current: The larger the resistance value is, the smaller the peak breakdown current will be. With the increase of resistance value, the decline of the peak breakdown current will slow down.

In this paper, a breakdown model of aged components in the container group is constructed for the breakdown fault of aged capacitors. The Mallet algorithm is used to decompose the strength data and convert it into electrical signals. Suppress overvoltage breakdown magnetizing inrush current and complete the detection of overvoltage breakdown of high voltage shunt capacitor banks. The result of the simulation experiment verifies that the detection deviation of the proposed method is very small compared with the actual monitoring result and the simulation result, which indicates that the proposed method has certain practical value in engineering.

2. Over-voltage breakdown detection of aged HV shunt capacitor banks

2.1. The breakdown model of aging components in the container group was established

When the aged element of the HV shunt capacitor bank operates under too high a voltage, the dielectric dissociation increases, and partial discharge may occur, which will increase the dielectric loss and lead to a dielectric breakdown in serious cases. The damage to the capacitor in operation is analyzed. The typical damage of capacitance aged element is the electric breakdown, and the fault feature is a short circuit. Assume that the running capacitor has a breakdown failure of an internal capacitance aged element. It is usually the individual components inside the capacitor that break down first, and the faulty component that breaks down becomes short-circuited, causing the faulty capacitor to lose a capacitor string. Suppose that the capacitance of a single capacitor is C. The total number of internal capacitance aging components in series is m series (4 strings in this paper). If the faulted capacitor has a series breakdown and the outer fuse is not fusing in time, the equivalent circuit of the faulted capacitor is shown in Figure 1.

2.2. Breakdown sequence of capacitor overvoltage

The over-voltage of high voltage shunt capacitors in different periods is realized according to a certain time sequence. Not in the same period, over-voltage said the timing of Figure 2. At the initial stage, the HV shunt capacitor is powered on, and the digital signal processor performs the reset operation. At this point, it is necessary to disconnect the contacts of power relays K_1, K_2 connected to the HV shunt capacitor, and complete the initialization of different modules. In the second stage, the shunt capacitor enters the standby state. During this period, the SHUNT capacitor continuously detects the DC voltage of the HV shunt capacitor. When the DC voltage of the HV SHUNT capacitor circuit is greater than the high limit or less than the low limit, the operation starts from the initial stage again. Assuming that the DC voltage in the standby stage is always normal, the third stage will be entered. Relay contacts and K_2 are closed, the voltage and frequency of the HV shunt capacitor are detected, and the RMS value of the shunt capacitor voltage is calculated. After the delay time T_s B, the effective value of capacitor output frequency and voltage is determined. Assuming that both items are in the normal range at this time, then the contact M is closed, and the HV shunt capacitor enters the power generation state after the completion of overvoltage over the same period. Assuming that the frequency and voltage of the network are abnormal, the HV shunt capacitor enters the initial stage.

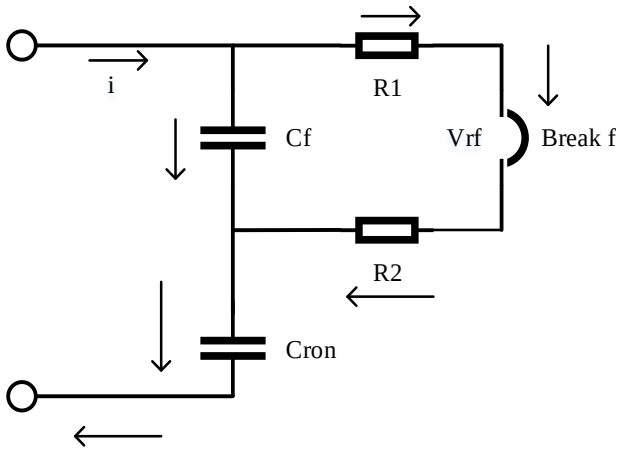

Figure 1. Fuse fusing capacitor inside not outside string element breakdown equivalent figure

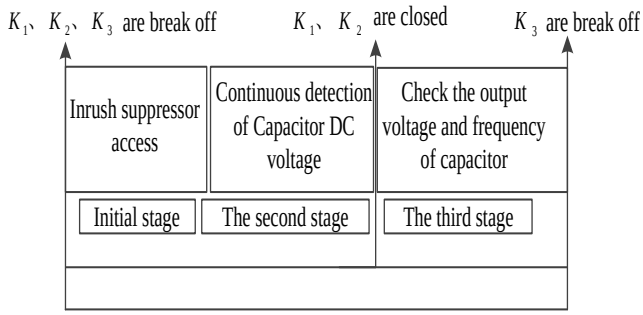

Figure 2. The over-voltage sequence of high voltage shunt capacitor in different periods

2.3. Breakdown strength data collection

Prior to data acquisition, the annual load status of the capacitor bank material needs to be evaluated. Unit vector iterative search for each subregion of aging element material, and the iterative search objective function is:

$$E_M = \sum_{t=1}^{T}\sum_{i=1}^{N}\left[\alpha_i + \beta_i P_{i,t} + \gamma_i P_{i,t}^2 + \xi_i \exp(\varphi_i P_{i,t})\right] \quad (1)$$

Where, α_i, β_i, γ_i, ξ_i, and ϕ_i are the material loss Angle coefficients of conventional unit i capacitor bank elements; T for collecting time, divided into 24 hours a day, each time for one hour; $P_{i,t}$ refers to the micronized impurities of a unit i in the t period. The material fuel cost and annual load condition compensation of the aged components in the region were taken as the total cost of the breakdown strength data [5]:

$$F_C = \sum_{t=1}^{T}\sum_{i=1}^{N}(a_i + b_i P_{i,t} + c_i P^2{}_{i,t}) + \sum_{t=1}^{T}\left(\frac{1}{\eta_D} P_{Dch,t} K_t \Delta t + \frac{1}{2} W_d \lambda^{Dch} P_{Dch,t} \Delta t\right) \quad (2)$$

Where, a_i, b_i and c_i are the environmental cost coefficients of the conventional unit i; η_D is the discharge efficiency of capacitor bank elements; $P_{Dch,t}$ is the discharging power of the elements of the capacitor bank at the time; K_t is the electricity price at time t; Δt is the discharge period; W_d is the discharge loss coefficient of capacitor bank elements; λ^{Dch} is the discharge mechanical damage coefficient of capacitor bank components. Taking the daily load variance as the safety index of capacitor bank component materials, the average load of 24 time periods in a day is obtained as follows:

$$\overline{P} = \frac{1}{T}\sum_{t=1}^{T}(P_{D,t} + P_{Ch,t} - P_{W,t} - P_{Dch,t}) \quad (3)$$

By obtaining the average load of aging component materials, the data signal acquisition function of the material breakdown strength of capacitor bank components is obtained:

$$L_V = \sum_{t=1}^{T}(P_{D,t} - \frac{P_{W,t}}{E_M} + \frac{F_C}{P_{Dch,t}})^2 \overline{P} \quad (4)$$

Where, $P_{D,t}$ is the current load demand of aging element materials at a time t; $P_{W,t}$ is the breaking elongation of capacitor bank elements at t a time; $P_{Ch,t}$ is the depolarizing power of the material of the capacitor bank element at t a time.

Through the capacitor set of components material breakdown strength data acquisition function, can be a variety of biological damage and pollution degree to detect index classification data such as data collection[6].On the basis of obtaining the breakdown strength data of capacitor bank components, the signal conversion of the breakdown strength data is conducted.

2.4. Breakdown of strength data signal conversion

On the basis of data collection of material breakdown strength of capacitor bank components, signal conversion is carried out on the collected data. Mallet algorithm is used to decompose the data and reconstruct the decomposed data [6]. In order to eliminate the component material breakdown strength data of the capacitor bank will cause the deviation of the test result. The data on the material breakdown strength of capacitor bank components are processed. Firstly, the data of material breakdown strength of capacitor bank components are decomposed by wavelet, and the data of breakdown strength is converted by signal, and the wavelet is selected. The decomposition level N is calculated, and the breakdown strength data of capacitor bank elements are decomposed into N layers. The wavelet function needs to select an orthogonal wavelet, and the signal conversion formula of the breakdown strength data is as follows:

$$X(e^{j\omega}) = \sum_{n=-\infty}^{\infty} x(n)e^{-j\omega n}L_V \quad (5)$$

Where, $x(n)$ is the breakdown intensity data signal; $X(e^{j\omega})$ represents a complex number, and the negative number varies with the angular frequency, and the negative number is used to represent the frequency domain signal of the breakdown intensity data; ω is distributed between $(-\infty, +\infty)$ [6-7].

Secondly, the high-frequency coefficients in the breakdown strength data of capacitor bank components are detected to reduce the deviation: The breakdown strength data in the N layer are processed with a high-frequency coefficient [8-9].

Finally, one-dimensional wavelet reconstruction is carried out for the breakdown strength data: The low-frequency coefficients in the N layer breakdown strength data and the processed high-frequency coefficients are taken as the basis. The breakdown strength data is reconstructed by a one-dimensional wavelet transform [9].

$$S_t = S_{t-1} + \eta_c P_{Ch,t}\Delta t - \frac{1}{\eta_D}P_{Dch,t}\Delta t - S_{Trip,t} \times X(e^{j\omega}) \quad (6)$$

$$S_{Trip,t} = \Delta S \times L \quad (7)$$

$$S_{\min} \le S_t \le S_{\max} \quad (8)$$

Where, η_c is the material detection efficiency of aging components, and S_t is the mechanical damage coefficient in the period t; $S_{Trip,t}$ is the material detection deviation of capacitor bank elements in the period t; ΔS is the average mechanical damage coefficient per unit distance; L is the breakdown strength; $S_{\min}$ and $S_{\max}$ are the upper and lower limits of detection indexes respectively.

Through the above operation, the parts of the material breakdown strength data of the capacitor bank elements that will cause the deviation of the test results are eliminated [10]. The online test result of material breakdown strength of capacitor bank components is more accurate.

2.5. Overvoltageltage breakdown inrush current suppression

The over-voltage breakdown inrush current suppressor of high voltage shunt capacitor is constructed by combining the second-order under damping circuit and the voltage divider. It is connected to the third winding of the capacitor to ensure that the voltage amplitude on different windings of the capacitor is different, but the phase is the same in order to eliminate the inrush current that occurs in different over-voltage stages of the HV shunt capacitor. The specific process is described as follows:

In the third winding of high voltage parallel capacitor and power connection between the inrush current limiter. Disconnect the main winding of the shunt capacitor on the low-voltage side of the transformer and energize the third winding of the capacitor with an inrush current suppressor. Steady-state alternating flux is generated in the transformer core in parallel with the capacitor:

$$\psi_2 = -\Phi_m \cos(\omega t + \alpha) \quad (9)$$

Where, α is over-voltage Angle, Φ_m is excitation inductance, ω is capacitor reactance, and t is capacitor running time.

On the basis of the formula (1), implementation of capacitor main winding over-voltage electricity. Without considering the active power loss of the HV shunt capacitor, the relationship between excitation voltage u and core flux ψ in the equivalent circuit of the capacitor is as follows:

$$\left\{u=\sqrt{2}U_m\sin(\omega t+\alpha)=d\psi/dt\right. \tag{10}$$

Where, u represents the capacitor's power supply side voltage, U_m represents the electrified signal of the gate coil of the HV shunt capacitor, d represents the iron core loss in the instant of the capacitor's over-voltage breakdown, dt represents the primary side leakage inductance, and the iron core flux chain ψ can be expressed as follows:

$$\psi=-\Phi_m\cos(\omega t+\alpha)+C \tag{11}$$

Where, C represents the capacitance value.

The flux linkage in the iron core of the HV shunt capacitor at different over-voltage periods is conserved, then:

$$-\Phi_m\cos(\omega t+\alpha)\Big|_{t=t_0}+C=\cos(\omega t+\alpha) \tag{12}$$

Where, $t=t_0$ represents the initial running time of the capacitor, then the magnetic bias in the iron core of the HV shunt capacitor at the moment of over-voltage breakdown is:

$$\psi_r=C=0 \tag{13}$$

The transient process of the HV shunt capacitor can be avoided by the above process. The third winding is disconnected at any time after the overvoltage breakdown of the HV shunt capacitor. At this point, there is no effect on the main magnetic circuit of the shunt capacitor, and the steady-state operation can be entered. The inrush current suppressor is realized by a second-order under a damped system. The main reason for using this system is that the characteristic roots of the transfer function of the second-order under a damped system are a pair of conjugate complex roots. Only the damping ratio of the second-order under a damped system needs to be set effectively. It can track the input voltage frequency and phase of each circuit of the HV shunt capacitor. The purpose of restraining the inrush current in each loop is realized. The input voltage source of the HV shunt capacitor is set as follows:

$$u_i=\sqrt{2}U_m\sin(\omega t+\alpha) \tag{14}$$

The corresponding expected output voltage of the second-order under a damped system can be expressed by the following formula:

$$u_0=\sqrt{2}U_m[1-\exp(-t/T)]\sin(\omega t+\alpha) \tag{15}$$

Where, T is the time constant. The input signals $U_i(s)$ and output signals $U_0(s)$ of each circuit of the HV parallel capacitor are Laplace transform [11]. There are:

$$\begin{cases}U_i(s)=\sqrt{2}U_m\omega\dfrac{2}{s^2+\omega^2}\\ U_0(s)=\sqrt{2}U_m\left(\dfrac{2}{s^2+\omega^2}-\dfrac{1}{(s+1/T)+\omega^2}\right)\end{cases} \tag{16}$$

Where, s stands for sinusoidal current. The transfer function of the second-order under a damped system can be obtained from the above equation:

$$H(s)=U_0(s)/U_i(s) \tag{17}$$

By combining formula (8) and formula (9), it can be known that the transmission function of the second-order under a damped system is a function of α and T, and the variation interval of α is given by using the following formula:

$$\begin{cases}\alpha_{\min}\le\alpha\le\alpha_{\max}\\ \alpha_{\min}=0\\ \alpha_{\max}=2\pi\end{cases} \tag{18}$$

Where, $\alpha_{\min}$ and $\alpha_{\max}$ respectively represent the maximum and minimum over-voltage angles.

Based on the above considerations, the value T should be appropriately increased: (1) When the value is large, the influence α can be minimized; When the value is small, the above second-order under a damped system can be regarded as an equivalent second-order system, and the equivalent second-order system has a lower design cost. (2) By increasing the value T, the steady rise of voltage amplitude on the third winding of the HV shunt capacitor can be guaranteed. The constant variation of the voltage amplitude at the output end of the capacitor leads to the change in the magnetic flux of the iron core, which reduces the possibility of causing the inrush current of the capacitor. The transfer function given in formula (9) is simplified, then:

$$H'(s)=1-\frac{s^2+\omega^2}{(s+a)^2+\omega^2} \tag{19}$$

According to the design scheme of capacitor in surge suppressor described in the above formula, appropriate HV shunt capacitors, inductors and resistors are selected by the following formula to control the control characteristics required by different over-voltage of HV shunt capacitors.

$$\begin{cases}\dfrac{R_2}{L}=\dfrac{2}{T}\dfrac{U_{2N}}{U_{3N}}\\ \dfrac{R_1+R_2}{L}=\dfrac{2}{T}\\ \dfrac{1}{LC}=\left(\dfrac{1}{T}\right)+\omega^2\end{cases} \tag{20}$$

Where, U_{2N} and U_{3N} respectively represent the corresponding rated capacitance values of the capacitor two-

phase winding and three-phase winding, L representing the inductance and $R_1 = R_2 = R$ represents the resistance.

2.6. Parameter condition and detection of the over-voltage breakdown of high voltage shunt capacitor

Suppose that U_T the effective value of the primary voltage of the isolation transformer during the grid-connected power generation stage of the high-voltage parallel capacitor I_L is the effective value of the current when the grid-connected power generation is at the maximum power and m is the capacitor circuit regulation. The vector triangle relationship of the high-voltage shunt capacitor is given by the following formula [12]:

$$mAU_D = \sqrt{U_T^2 + [\omega_f (L_{m1} + L_{m2}) I_L]^2} \quad (21)$$

Where, ω_f is the speed, L_{m1} and L_{m2} are the inductance values of the shunt capacitor circuit, and U_T^2 is the open-circuit voltage of the shunt capacitor

$$U_D = \frac{\sqrt{2}\sqrt{U_T^2 + [\omega_f (L_{m1} + L_{m2}) I_L]^2}}{mA} \quad (22)$$

It can be seen from the above formula that when the high-voltage shunt capacitor outputs the equivalent maximum power, the smaller the m value is, the higher the corresponding open-circuit voltage of the capacitor is, and the higher the voltage borne by the high-voltage shunt capacitor.

It is assumed that the DC voltage of the high voltage shunt capacitor is low at the current stage, and m reaches the maximum, and has no output power. At this time, the voltage can only maintain the operation of the shunt capacitor itself. At this time, formula (22) can be converted into [13]:

$$mU_{D\min} = \sqrt{2}U_T \quad (23)$$

$U_{D\min}$ is used to describe the minimum open-circuit voltage of the shunt capacitor.

According to relevant certification standards [14], the normal operation output frequency range of a high-voltage shunt capacitor is 48.5-50.5hz, and the range of single AC voltage is 186-240v. These two factors can constitute the AC side parameter conditions of the over-voltage breakdown of a high-voltage shunt capacitor. The shadow area given in Fig. 3 is used to characterize the over-voltage breakdown area of the shunt capacitor.

When the relay contacts K_1 and K_2 are closed, the high-voltage shunt capacitor should detect the effective value and frequency of the grid voltage in different periods. When the voltage frequency and effective value of different periods are in the shaded area in Fig. 3, it indicates that the power grid is in normal operation at this time, and the shunt capacitor is allowed to close the power relay contact K_3, and the high-voltage shunt capacitor will turn into the power output state after full over-voltage, otherwise, the contact will be disconnected Point K_1, K_2 capacitor into standby mode[15]. The output voltage of the high-voltage capacitor is detected after closing contacts K_1 and K_2. In order to make the output voltage stable enough time, T_d is required to be long enough. After many times of debugging, $T_d = 80ms$ is selected. After T_d a period, the average output voltage and whether the power grid is normal are determined. If the current period is normal, K_3 is closed, and contacts K_1 and K_2 are disconnected.

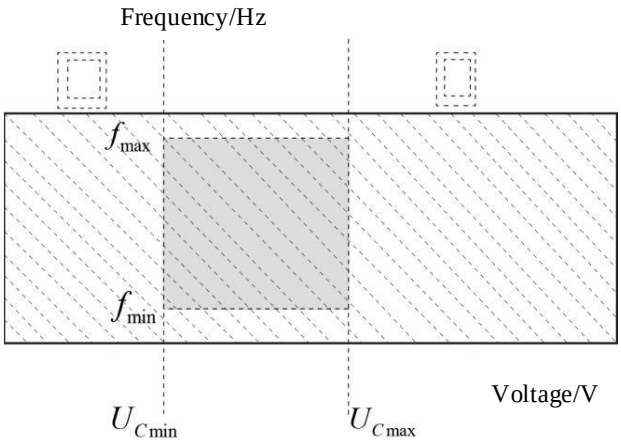

Figure 3. Over-voltage breakdown area of high voltage shunt capacitor

2.7 Construction of online detection platform

According to the data processing results, an online detection platform for the breakdown strength of capacitor bank components is constructed. The platform is mainly composed of a signal processing unit, signal receiving unit, and signal transmitting unit. The narrow pulse signal is transmitted from the signal transmitting unit to the capacitor bank component material. In the capacitor bank component material, the narrow pulse signal will continuously propagate and be affected by the breakdown strength of the capacitor bank component material, thus generating the reflection pulse corresponding to the breakdown strength. The signal receiving unit is set at the other end of the capacitor to receive the data and transmit the signal. The reflected pulse and transmitted pulse emitted by the unit are stored in the buffer of FPGA, and the data is transmitted to the upper computer by the serial port of FPGA. The reflected pulse is analyzed by the detection algorithm in the upper computer, and the breakdown strength of the capacitor bank component material corresponding to the reflected pulse is obtained, so as to realize the online detection of the breakdown strength of the capacitor bank component material. The specific detection process is shown in Figure 4.

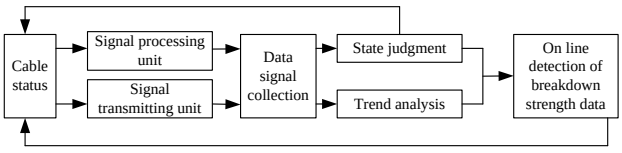

Figure 4. Specific detection process

Among them, the hardware of the signal processing unit mainly includes a controller, analogue-to-digital conversion chip, and upper computer. The model of the controller is HDL Verilog, and the controller can work with various simulation tools; the specific model of analogue-to-digital conversion chip is AD7810, which is a low-power A/D conversion acquisition chip, which is powered by a single power supply, has the highest sampling frequency of 100kHz and serial data interface, and can be connected with the upper computer to realize the hardware function of the signal processing unit. The software of the signal processing unit is the breakdown strength detection unit, which mainly uses the detection algorithm to analyze the reflected pulse so as to realize the detection of the breakdown strength of capacitor bank components.

The signal receiving unit mainly includes a step delay chip and a programmable digital delay pulse receiver. The specific model of step delay chip is AD9501, which can support both CMOS level and TTL level and can achieve the minimum delay time of 10ps and the maximum trigger frequency of 50MHz; the programmable digital delay pulse receiver is mainly responsible for the reflection pulse corresponding to the breakdown strength Receive.

The signal transmitting unit mainly includes a delay pulse trigger circuit and programmable digital delay pulse transmitter. The delay pulse trigger circuit mainly uses an A/D conversion chip to trigger the delay pulse, which is mainly composed of a voltage comparator, step wave generator, and oblique wave generator; the programmable digital delay pulse transmitter is mainly responsible for transmitting narrow pulse signal. Through the signal processing unit, the signal receiving unit, and the signal transmitting unit, the online detection of the breakdown strength of the capacitor bank components is realized.

3. Experimental results and analysis

3.1 Output results of aging over-voltage breakdown detection of high voltage shunt capacitor bank components

Simulation calculation of capacitor breakdown in a series of time, the solid dielectric inside the capacitor is only a few tens of microns film, the breakdown of capacitor aging components belongs to voltage breakdown. The breakdown of a c-phase capacitor is simulated by the simulation model. The breakdown of capacitor aging components occurs at the time when the c-phase bears the peak voltage. The phase of the sinusoidal current on the capacitor is 90° ahead of the voltage phase at both ends of the capacitor. The current breakdown phase is approximately 0. In the simulation calculation. When the C phase is set at 9.8ms, the voltage at both ends of the capacitor is close to the peak value of phase voltage. The breakdown process is simulated as the control switch is closed. The breakdown point of a series of components of the capacitor is equivalent to the series branch of small resistance and small inductance. The main observed quantities are the current of the branch where the capacitor is broken down and the voltage and current of the three-phase capacitor circuit. Figure 5 shows the current waveform on the breakdown capacitor branch during the breakdown process. Figure 6 shows the voltage waveform on the three-phase capacitor. The positive peak voltage waveforms in the Figure are B, C, and A-phase capacitors respectively. The voltage on the c-phase capacitor drops rapidly and the voltage drop is 392V. The breakdown current waveform and voltage waveform of the three-phase capacitor in the process of over-voltage breakdown are shown in Fig. 5 and Fig. 6.

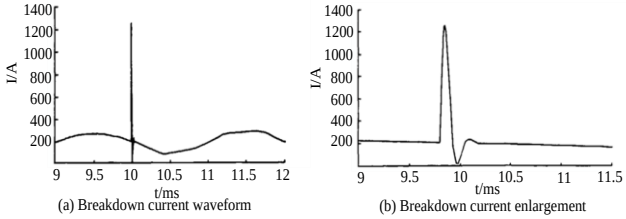

Figure 5. The current waveform on the breakdown capacitor branch

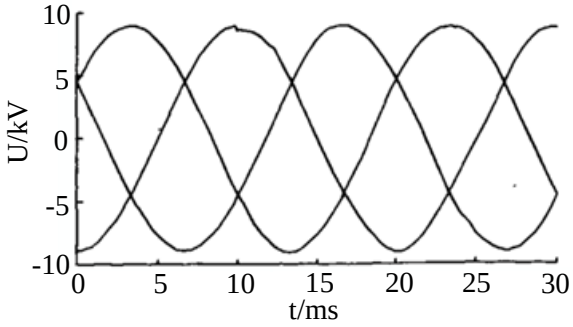

Figure 6. The voltage waveform of the three-phase capacitor during the breakdown

3.2 Comparative analysis of simulation results and fault data recorded by a monitoring device

In order to verify the effectiveness of the proposed method, the proposed method is used to detect the over-voltage breakdown process of aging components of a real shunt capacitor bank, and the results are compared with the real monitoring results of the monitor. In order to monitor the failure process of capacitor bank, a power supply bureau in Guangdong Province. A high voltage shunt capacitor online monitoring device is installed on several capacitor banks with frequent faults. It can record a variety of fault data of the capacitor bank in time, including current and phase voltage data of each capacitor branch. The data sampling frequency of the monitoring device is 10 kHz. It can record various waveforms of the breakdown process quickly. Two breakdowns occurred in the capacitor. The effective value of capacitor C8 current increased from 55.2A to 83.4A. The online monitoring device of the shunt capacitor shows its fault and gives an alarm. The current of other capacitors has no obvious change. The effective value of the C8 current of the capacitor bank increased to 134.4A again after the capacitor bank was maintained in this working state for about 75 min. The current of other capacitors is basically unchanged. After the capacitor bank is in this state for about 200 ms, the capacitor bank is removed from the system. After the failure of the capacitor bank, it is detected. Faulty capacitor C. The variation of capacitance is 53.6 μF. According to the fault current records and post fault detection results of each

capacitor branch, it can be inferred that the first increase of C8 current is the performance of a series of capacitor aging components in its internal four strings, and the second current increase is the performance of a series of capacitor aging components in the remaining three strings. At this time, an unbalanced current is detected by neutral line unbalance protection. After 220 ms of protection setting value. The relay protection of capacitor bank acts. Make the vacuum circuit breaker of the capacitor bank open the capacitor bank at 740ms. Fig. 7 is the fault recording of the breakdown of the internal capacitance aging element of a capacitor in phase C recorded by the monitoring device and the detection results of the method proposed in Fig. 8.

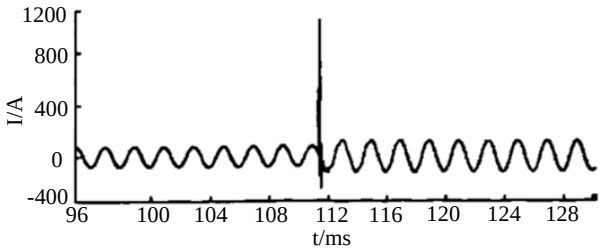

Figure 7. Waveform recording of monitoring device

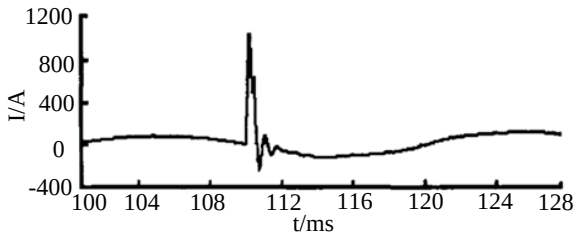

Figure 8. Test results of the proposed method

It can be seen from the fault waveform in figure 8. When a series of capacitor aging components are broken down, the current of the capacitor branch is about 0 before the breakdown, and then there is a high-frequency discharge oscillation for about 2 ms. The discharge front is very steep, and the first peak value is about 1050A. In terms of breakdown current peak value, oscillation frequency, and transition time, the above theoretical and simulation analysis are in good agreement with fault waveform records.

4. Conclusions

As the main reactive power compensation device of the substation, the shunt capacitor bank is in a high temperature and high voltage environment for a long time. Due to insulation aging and other reasons, the dielectric strength of the capacitor will gradually decrease. In addition, due to the instantaneous over-voltage between the electrodes of the capacitor, the weak components inside the capacitor may break down, resulting in capacitor damage. This paper presents an analysis method of the aging over-voltage breakdown of high voltage shunt capacitor banks. The simulation results show that the detection results of the proposed method are identical to the actual detection results, and the application performance is good.

Ethical issue

The authors are aware of and comply with best practices in publication ethics, specifically with regard to authorship (avoidance of guest authorship), dual submission, manipulation of figures, competing interests, and compliance with policies on research ethics. The authors adhere to publication requirements that the submitted work is original and has not been published elsewhere in any language.

Data availability statement

Data sharing is not applicable to this article as no datasets were generated or analyzed during the current study.

Conflict of interest

The authors declare no potential conflict of interest.

References

[1] Ghossein N. E., Sari A., Venet P., Effects of the hybrid composition of commercial lithium-ion capacitors on their floating aging, IEEE Transactions on Power Electronics, 2019, 25(3), 115-126.

[2] Kamyab, H., Naderipour, A., Jahannoush, M., Abdullah, A., Marzbali, M. H. (2022). Potential effect of SARS-CoV-2 on solar energy generation: Environmental dynamics and implications. Sustainable Energy Technologies and Assessments, 52, 102027.

[3] Azizi A., Logerais P.O., Omeiri A., et al., Impact of the aging of a photovoltaic module on the performance of a grid- connected system, Solar Energy, 2018, 174(15), 445-454.

[4] Liao L., Gao H., He Y., Xu X., You F., Fault diagnosis of capacitance aging in DC link capacitors of voltage source inverters using evidence reasoning rule, Mathematical Problems in Engineering, 2020, 2020(9), 1-12.

[5] Bai Y., He H., Li J., Li S., Wang Y., Yang Q., Battery anti-aging control for a plug-in hybrid electric vehicle with a hierarchical optimization energy management strategy, Journal of Cleaner Production, 2019, 237(10), 1-16.

[6] Mejdoubi A.E., Chaoui H., Sabor J., Gualous H., Remaining useful life prognosis of supercapacitors under temperature and voltage aging conditions, IEEE Transactions on Industrial Electronics, 2018, 65(5), 4357-4367.

[7] Xu C., Chen Z., Cheng K.W.E., Wang X., Ho H., A supercapacitor-based method to mitigate over-voltage and recycle the energy of pantograph arcing in the high speed railway, Energies, 2019, 12(7), 259-271.

[8] Islam M.M., Sutanto D., Muttaqi K.M., Protecting PFC capacitors from over-voltage caused by harmonics and system resonance using high temperature superconducting reactors, IEEE Transactions on Applied Superconductivity, 2019, 29(2), 100-115.

[9] Yang Q., Yin L., Liu H., Wang K., Huang J., Measurement of Lightning-Induced over-voltage in power distribution lines using ceramic-capacitor insulator, IEEE Transactions on Electromagnetic Compatibility, 2019, 23(9), 1-8.

[10] Navaei M., Abdoos A.A., Shahabi M., A new control unit for electronic ferroresonance suppression circuit in capacitor voltage transformers, International Journal

of Electrical Power and Energy Systems, 2018, 99(1), 281-289.

[11] Han P., He X., Zhao Z., Yu H., Wang Y., DC-link capacitor voltage balanced modulation strategy based on three-level neutral-point-clamped cascaded rectifier, Journal of Power Electronics, 2019, 19(12), 89-106.

[12] Yao Z., Zhang Y., Hu X., MOSFET-clamped three-level converters without flying capacitor, International Transactions on Electrical Energy Systems, 2020, 30(2), 1221-1235.

[13] Sanjeevikumar P., Mahajan B., Pandav M., Blaabjerg F., Fedák V., An original transformer and switched-capacitor (T & SC)-based extension for DC-DC boost converter for high-voltage/low-current renewable energy applications: hardware implementation of a new T & SC boost converter, Energies, 2018, 11(4), 783-795.

[14] Farkoush S.G., Wadood A., Khurshaid T., Kim C.H., Rhee S.B., Minimizing static VAR compensator capacitor size by using SMC and ASRFC controllers in smart grid with connected EV charger, International Journal of Electrical Power and Energy Systems, 2019, 107(5), 656-667.

[15] Yamazaki H., Kurui Y., Saito T., et al., CMOS-embedded high-power handling RF-MEMS tunable capacitor using quadruple series capacitor and slit with dielectric bridges structure, Jpn. J. Appl. Phys, 2018, 57(10), 1002-1013.